Defect-induced activation of symmetry forbidden infrared resonances in individual metallic nanorods

F. Neubrech,[1,a)] A. Garcia-Etxarri,[2,a)] D. Weber,[1] J. Bochterle,[1] H. Shen,[3] M. Lamy de la Chapelle,[4] G. W. Bryant,[5] J. Aizpurua,[2] and A. Pucci[1]
[1]*Kirchhoff-Institute for Physics, University of Heidelberg, 69120 Heidelberg, Germany*
[2]*Donostia International Physics Center (DIPC), Centro de Física de Materiales CSIC-UPV/EHU, 20018 Donostia, Spain*
[3]*Institut Charles Delaunay, FRE CNRS 2848, Université de technology de Troyes, 10010 Troyes Cedex, France*
[4]*Laboratoire CSPBAT, FRE 3043, UFR SMBH, Université Paris 13, 93017 Bobigny, France*
[5]*National Institute of Standards and Technology, Gaithersburg, Maryland 20899, USA*

(Received 14 April 2010; accepted 28 April 2010; published online 26 May 2010)

We report on the observation of second-order infrared (IR) plasmon resonances in lithographically prepared gold nanorods investigated by means of far-field microscopic IR spectroscopy. In addition to the fundamental antennalike mode, even and odd higher order resonances are observed under normal incidence of light. The activation of even-order modes under normal incidence is surprising since even orders are dipole-forbidden because of their centrosymmetric charge density oscillation. Performing atomic force microscopy and calculations with the boundary element method, we determine that excitation of even modes is enabled by symmetry breaking by structural deviations of the rods from an ideal, straight shape. © *2010 American Institute of Physics*.
[doi:10.1063/1.3437093]

Antennalike metal nanoparticles offer a large variety of applications in today's technologies because their plasmonic properties and thus their optical excitations can be tuned over a broad frequency range. Of special interest is the huge near-field enhancement at resonance because it enables extraordinarily sensitive detection of molecules.[1–7] The exact frequency of the plasmonic resonance depends not only on the kind of metal (described by the plasma wavelength λ_P) but also on length L, diameter D (or the spatial cross section), and overall shape of the particle.[8–12] Considering a cylindrical antenna with $L>D$ and with very good metallic conductivity, the relation between L and the fundamental optical resonance wavelength λ_{res} is well described by the linear relation,[11]

$$2L = n_1 + n_2 \lambda_{res}/\lambda_P. \quad (1)$$

The coefficients n_i depend on geometry of the nanorod and on the dielectric background of the environment (with effective refractive index, e.g., Ref. 10). From the mid to far infrared (IR), for gold nanorods with micrometer lengths (and $L/D>10$), n_1 becomes very small and $\lambda_{res}=2\lambda_p n_2^{-1} L=bL$ which is a relation like that of an ideal antenna where $b=2$. Besides the strong fundamental ($l=1$) mode, such nanoantennas also exhibit multipolar ($l>1$) resonances at λ_{res}/l.[9,12–14] Only multipolar modes with an antisymmetric charge distribution (odd l) can be optically excited at normal incidence of light because their total dipole moment does not vanish.[13,15] In contrast to these bright modes, plasmonic excitations with a centrosymmetric charge distribution (even l) (Ref. 16) cannot be excited under such conditions and are known as dark modes. Dark modes become visible when some type of symmetry-breaking is present. At oblique incidence, symmetry-breaking arises due to retardation effects and excitation of the dark modes becomes possible because of the phase difference of the incoming wave at the two nanorod ends. Indeed, such behavior was observed in nanorods[14,15,17] and also in other metallic nanostructures.[18] In addition, dark modes are observed in spectroscopic studies of complex multimer structures.[19–22] In this paper we report on the appearance of dipole-forbidden second-order modes ($l=2$) in the IR spectra of some single gold nanorods under normal incident radiation and we identify the origin of this effect.

As done in Refs. 4 and 12, homogeneous nanorod arrays were prepared by electron beam lithography on zinc sulfide (ZnS) substrates. The distances between single nanorods were chosen to be 5 μm (30 μm) in both directions to suppress the near-field interaction. L varies from 0.5 to 2.5 μm. The width w and the height h are about 60 nm in 5 μm arrays; $h\approx 100$ nm in 30 μm arrays. By use of scanning electron microscopy (SEM) and atomic force microscopy (AFM) we determined the actual size and shape of the nanorods (for each rod in the 30 μm arrays and for a statistically relevant selection in the 5 μm arrays, respectively). Microscopic IR spectroscopy (with an aperture diameter of 8.3 μm and 16.7 μm, respectively) was performed using radiation both from a synchrotron light source (Angström source Karlsruhe, ANKA) and from a thermal light source (globar), measured with a mercury–cadmium detector (MCT).[7,10,12] The reference measurements were taken on the bare substrate at least 30 μm away from nanorods. IR transmittance spectra were recorded by acquisition of at least 1000 scans in the spectral range from 700 to 7000 cm^{-1} with a resolution of 8 cm^{-1}.

The example spectra in Fig. 1 feature the fundamental plasmonic band for parallel polarization; the plasmonic signal for perpendicular polarization remains below the noise

a)Authors to whom correspondence should be addressed. Electronic addresses: neubrech@kip.uni-heidelberg.de and aitzol_garcia@ehu.es.

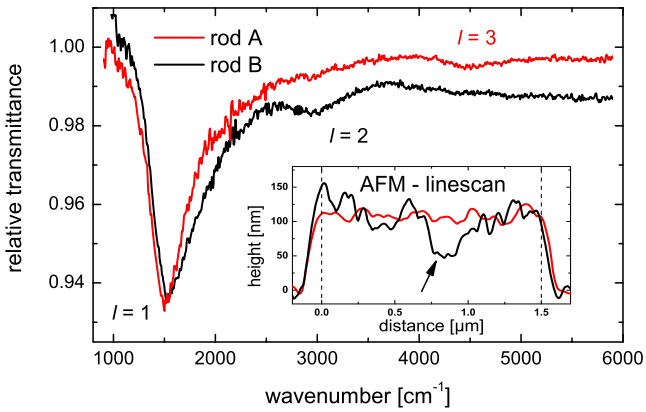

FIG. 1. (Color online) Relative IR transmittance spectra of two similarly prepared nanorods (A and B) with $L \approx 1500$ nm, $w=60$ nm, and $h=100$ nm. The resonance order l is indicated. The inset shows AFM height profiles along the rod's long axis. The main defect of nanorod B is indicated with an arrow.

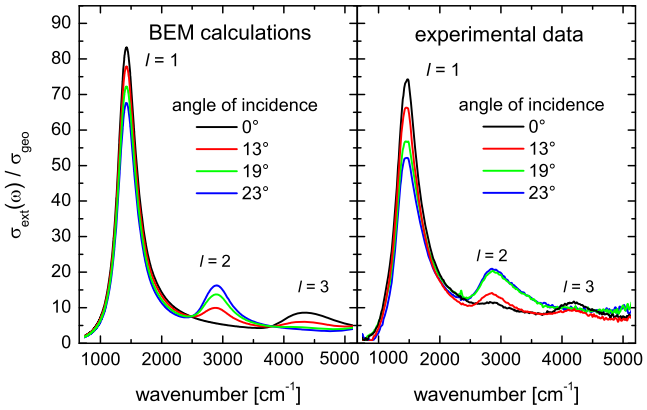

FIG. 3. (Color online) Experimental extinction cross section (σ_{ext}, derived from transmittance as in Refs. 10 and 12, normalized to the geometric cross section σ_{geo}) of a nanorod with $w \approx h \approx 60$ nm, compared to BEM calculations for a cylindrical nanorod ($D=68$ nm, $\pi D^2=4wh$) of the same length $L=1500$ nm for various incident angles α as indicated.

level. For various L, the optical resonance wavelength for $l=1$ follows Eq. (1) with $n_1 \approx 0$ and $\lambda_{res}=b(l=1)L \approx 4.6 \cdot L$ as can be seen in Fig. 2. In Fig. 1, not only does the fundamental resonance ($l=1$) appear in the spectrum but additional bands, probably higher order excitations, also show up. Surprisingly, a plasmonic band at twice the optical resonance wavenumber of the fundamental mode is observed in the spectra of some nanorods (for example nanorod B in Fig. 1). If $\lambda_{res}=b(l=1)L$ is compared to the experimental relations between the other resonances and L, their assignment to higher order resonances ($l=2,3$) becomes unambiguous, see Fig. 2 and inset with table.

Because both collection and condenser lens have a numerical aperture of 0.52, the incident IR radiation is not strictly incident along the normal direction and a small fraction of the light scattered away from the normal is detected. To identify clearly the effect of non-normal incidence of light on the appearance of the $l=2$ mode, we tilted the sample to various angles (30°, 45°, and 60° with an error of about ±5°) between the substrate normal and the direction of the incident light in air, which corresponds to angles of 13°, 19°, and 23° in ZnS according to Snell's law. As known from literature,[15,17,18] dark modes appear for such configurations

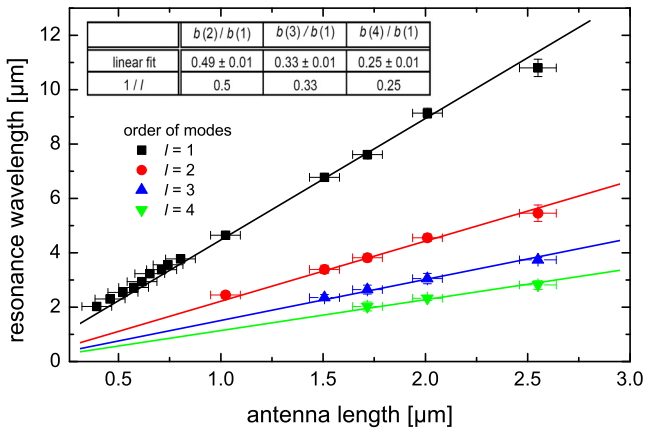

FIG. 2. (Color online) Relation between λ_{res} and length L for different orders l. The solid lines are linear fits of $\lambda_{res}=b(l)L/l$ to the experimental data with the fit parameter $b(l)$ for the lth order. The inset-table compares $b(l)/b(l=1)$ to the ideal ratio $1/l$. The error bars indicate the experimental error in the resonance frequency and length as estimated from SEM images.

because the incident electrical field is no longer constant along the length of the nanoantenna and phase shifts occur over the full nanorod length. For increasing incident angle, the coupling between the incident radiation and the dark modes becomes more efficient (up to a certain angle depending on the surrounding medium) while coupling to bright modes is less efficient.[15] We observe similar behavior for the IR antennas as shown in Fig. 3 where a quantitative comparison of extinction cross sections is given. To verify further these experimental results, we performed calculations using the boundary element method (BEM) (Refs. 9 and 23) for different angles of incidence. By means of BEM we solve Maxwell's equations for the scattering of a cylindrical gold nanorod (with bulk dielectric properties[24]) in an isotropic environment (with effective refractive index $n_{eff}=1.71$).[12] The computational results qualitatively show the appearance of the second-order mode and the decrease in intensity of bright modes for increasing incident angle. Good agreement between the experiments and the calculations is achieved for the various angles of incidence (see Fig. 3). The second-order mode clearly does not appear at normal incidence as experimentally observed for many of the nanorods (e.g., rod A in Fig. 1).

What other effect explains the unexpected appearance of dark modes of some nanorods in normal incidence experiments? Any possible asymmetric beam profile of the synchrotron radiation, which might also couple light to dark modes, can be excluded because measurements with a thermal light source show the same behavior. However, a deviation from the ideal shape of a perfectly smooth nanorod might break the symmetry of the collective charge oscillation. Therefore, we performed AFM height scans of various nanorods along their long axis (see inset of Fig. 1). Obviously, the nanorods differ in surface roughness: whereas nanorod A features a more or less smooth surface with steps of less than 10 nm, nanorod B exhibits several large steps with a height difference of up to 50 nm. Moreover, the largest step is away from the rod center so that the rod symmetry is clearly broken, which enables the appearance of the $l=2$ mode. The symmetry-breaking effect of defects is verified by BEM calculations using a simplified model of a defective cylindrical nanorod using a neck in the rod, offset from the rod center (see Fig. 4). The BEM calculations were per-

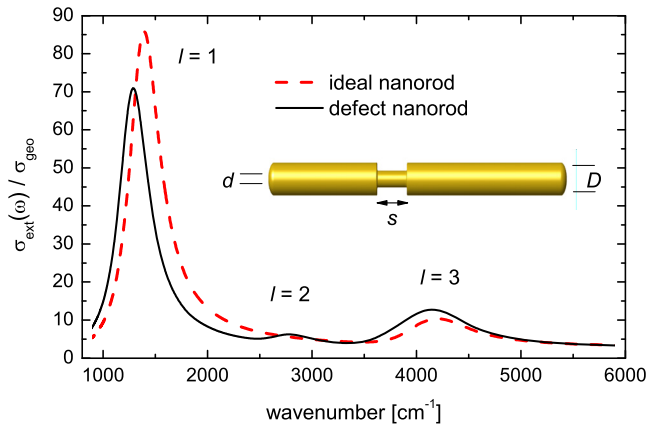

FIG. 4. (Color online) Simulated extinction spectra of an ideal (broken line) and an inhomogeneous (solid line) nanorod with $L=1500$ nm and $D=60$ nm. The detailed shape of the nanorod with defects is shown in the inset ($d=30$ nm, $s=100$ nm, the neck position is 155 nm away from the rod center).

formed as described before but now for normal incidence of light. With this neck, the second-order mode indeed appears clearly in the spectral signature of the rod (see Fig. 4). According to the calculations, the signal strength of the $l=3$ mode should be similar for nanorods A and B. However, above 3500 cm^{-1}, a broadband decrease in transmission is observed for nanorod B, which may originate from the multiple steps on the nanorod which are not accounted for in the model. Nevertheless, the calculations confirm that the experimental appearance of the second-order modes is induced by the presence of defects in the nanorod. The appearance of even-order modes under normal incidence can, therefore, be used as a fingerprint to detect the presence of inhomogeneities in micron-sized nanoobjects.

In conclusion, we observed dark modes in IR spectra of linear gold nanoantennas at normal incidence. The appearance of such dark modes could be clearly attributed to the presence of defects in the nanorod that break symmetry. This interpretation is proven conceptually by BEM calculations and corroborated in AFM studies. Such lithography defects may be induced by inhomogeneities in the substrate's surface (scratches, for instance) or imperfections arising from the preparation process for the nanorods. Therefore, the observation of even modes could be used as an indicator for the quality of nanorod arrays.

We gratefully thank P. Nordlander and acknowledge funding within the "Nanoantenna" collaborative European project (No. HEALTH-F5-2009-241818). We gratefully thank M. Süpfle, B. Gasharova, and Y.-L. Mathis for their support at ANKA. The authors from the University of Heidelberg, University of Troyes, and University of Paris 13 acknowledge financial support by the DAAD and Partenariat Hubert Curien Procope Program, the Egide Organisation, and the Conseil Régional de Champagne Ardenne. D.W. acknowledges financial support by the Heidelberg Graduate School of Fundamental Physics, F.N. acknowledges financial support by the FRONTIER project. J.A. and A.G.E. acknowledge financial support from National Project No. FIS2007-66711-C02-01 from the Spanish Ministry of Innovation and Science.

[1] S. M. Nie and S. R. Emory, Science **275**, 1102 (1997).
[2] E. Fort and S. Gresillon, J. Phys. D **41**, 013001 (2008).
[3] H. Wang, J. Kundu, and N. J. Halas, Angew. Chem., Int. Ed. **46**, 9040 (2007).
[4] J. Grand, M. Lamy de la Chapelle, J.-L. Bijeon, P.-M. Adam, A. Vial, and P. Royer, Phys. Rev. B **72**, 033407 (2005).
[5] L. Billot, M. Lamy de la Chapelle, A.-S. Grimault, A. Vial, D. Barchiesi, J.-L. Bijeon, P.-M. Adam, and P. Royer, Chem. Phys. Lett. **422**, 303 (2006).
[6] D. Enders and A. Pucci, Appl. Phys. Lett. **88**, 184104 (2006).
[7] F. Neubrech, A. Pucci, T. Cornelius, S. Karim, A. García-Etxarri, and J. Aizpurua, Phys. Rev. Lett. **101**, 157403 (2008).
[8] K. B. Crozier, A. Sundaramurthy, G. S. Kino, and C. F. Quate, J. Appl. Phys. **94**, 4632 (2003).
[9] J. Aizpurua, G. W. Bryant, L. J. Richter, F. J. García de Abajo, B. K. Kelley, and T. Mallouk, Phys. Rev. B **71**, 235420 (2005).
[10] F. Neubrech, T. Kolb, R. Lovrincic, G. Fahsold, A. Pucci, J. Aizpurua, T. W. Cornelius, M. E. Toimil-Molares, R. Neumann, and S. Karim, Appl. Phys. Lett. **89**, 253104 (2006).
[11] L. Novotny, Phys. Rev. Lett. **98**, 266802 (2007).
[12] F. Neubrech, D. Weber, R. Lovrincic, A. Pucci, M. Lopes, T. Toury, and M. Lamy de La Chapelle, Appl. Phys. Lett. **93**, 163105 (2008).
[13] J. R. Krenn, G. Schider, W. Rechberger, B. Lamprecht, A. Leitner, and F. R. Aussenegg, Appl. Phys. Lett. **77**, 3379 (2000).
[14] J. Dorfmüller, R. Vogelgesang, R. T. Weitz, C. Rockstuhl, C. Etrich, T. Pertsch, F. Lederer, and K. Kern, Nano Lett. **9**, 2372 (2009).
[15] G. Schider, J. R. Krenn, A. Hohenau, H. Ditlbacher, A. Leitner, F. R. Aussenegg, W. L. Schaich, I. Puscasu, B. Monacelli, and G. Boreman, Phys. Rev. B **68**, 155427 (2003).
[16] A. Pucci, F. Neubrech, J. Aizpurua, T. Cornelius, and M. Lamy de la Chapelle, in *One-Dimensional Nanostructures*, Springer Book Series: Lecture Notes on Nanoscale Science and Technology Vol. 3, edited by Z. Wang (Springer, New York, 2008), p. 175.
[17] G. Laurent, N. Félidj, J. Aubard, G. Lévi, J. R. Krenn, A. Hohenau, G. Schider, A. Leitner, and F. R. Aussenegg, Phys. Rev. B **71**, 045430 (2005).
[18] F. Hao, E. M. Larsson, T. A. Ali, D. S. Sutherland, and P. Nordlander, Chem. Phys. Lett. **458**, 262 (2008).
[19] P. Nordlander, P. Coubre, E. Prodan, K. Li, and M. Stockman, Nano Lett. **4**, 899 (2004).
[20] F. Hao, P. Nordlander, Y. Sonnefraud, P. V. Dorp, and S. A. Maier, ACS Nano **3**, 643 (2009).
[21] F. Hao, C. L. Nehl, J. H. Hafner, and P. Nordlander, Nano Lett. **7**, 729 (2007).
[22] H. Wang, D. Brandl, P. Nordlander, and N. J. Halas, Acc. Chem. Res. **40**, 53 (2007).
[23] F. J. García de Abajo and A. Howie, Phys. Rev. Lett. **80**, 5180 (1998); Phys. Rev. B **65**, 115418 (2002).
[24] E. D. Palik, *Handbook of Optical Constants of Solids* (Academic, New York, 1985).